Reaction dynamics of atomic chlorine with methane: Importance of methane bending and torsional excitation in controlling reactivity

S. Alex Kandel and Richard N. Zare
Department of Chemistry, Stanford University, Stanford, California 94305

(Received 3 August 1998; accepted 3 September 1998)

The reactions of atomic chlorine with CH_4 and CD_4 were studied at five collision energies ranging from 0.13 to 0.29 eV using resonance-enhanced multiphoton ionization of the CH_3 and CD_3 products. Core-extracted ion arrival profiles were used to determine methyl radical product speed distributions. The distributions contain products that are moving anomalously fast which energetically cannot result from the reaction of ground-state chlorine with ground-state methane. We attribute these products to reaction of ground-state chlorine with methane vibrationally excited in trace quantities into low-energy bending and torsional modes. Measurements of product spatial anisotropy are used to confirm this interpretation and to indicate that the possible reaction of spin–orbit excited chlorine is less important. These low-energy vibrations create large enhancements in reactivity over ground-state molecules, and consequently, vibrationally excited reagents dominate reactivity at low collision energies and contribute substantially at the highest collision energies studied. It is suggested that vibrationally excited reagents play an important role in the thermal kinetics of the reaction of chlorine with methane and may contribute significantly to explain the observed deviation from Arrhenius equation behavior. Scattering distributions of the products of both ground-state and vibrationally excited reactions are reported, and additional measurements of the internal state distributions of the CH_3 and CD_3 products reveal that the methyl radicals contain very little energy in rotation or vibration. © *1998 American Institute of Physics.* [S0021-9606(98)01646-8]

I. INTRODUCTION

The reaction of atomic chlorine with methane,

$$Cl+CH_4 \rightarrow HCl+CH_3,$$

is important in atmospheric processes as the dominant source of HCl in the stratosphere. Additionally, the reaction is interesting from a dynamical standpoint as a simple gas-phase reaction involving a polyatomic reagent and product; such reactions afford the possibility for extending traditional studies of atom-plus-diatom reactions to more complex systems. Past work in this laboratory has investigated the reaction of chlorine atoms with hydrocarbons[1–7] and detailed the effect on reactivity of C–H stretch vibrational excitation.[5–7] This paper concerns our most recent studies of the $Cl+CH_4$ and $Cl+CD_4$ reactions, in which we report state distributions and scattering of the CH_3 and CD_3 products as a function of collision energy. Furthermore, we provide evidence that excitation of the low-energy bending and torsional modes of the methane reagent results in significantly enhanced reactivity.

The $Cl+CH_4$ reaction is endothermic by 600 cm^{-1} (0.07 eV) and has a rate of 1.0×10^{-13} cm^3 $molecule^{-1}$ s^{-1} at 298 K.[8–10] Kinetic studies show that the reaction has non-Arrhenius behavior, and thus the thermal rate can be expressed only approximately in simple exponential form, $k(T)=Ae^{-E_a/kT}$. Consequently, determining the reaction's activation energy is not straightforward. An exponential fit to the data[9] yields a value of $[1.8\times10^{-11}$ cm^3 $molecule^{-1}$ $s^{-1}]$ $e^{-1580/T}$, and fits to low-temperature and higher-temperature data result in smaller or larger values, respectively. Calculations based on changes in zero-point energy indicate that the $Cl+CD_4$ reaction should be endothermic by 900 cm^{-1} (0.11 eV). In this paper, we report our investigations of these reactions over a range of well-defined collision energies from below the reactive barrier to significantly above it. Therefore, we are studying the types of collisions most likely to be responsible for reactivity under thermal conditions.

Our previous work concerning the reaction of atomic chlorine with CH_4 and CD_4 studied the HCl and DCl reaction products, and produced several results that are relevant to the current investigation.[3] First, we observed that the HCl and DCl products contain very little internal energy. HCl products possess on average 31 cm^{-1} of rotational energy, and DCl products possess 38 cm^{-1}; vibrational excitation is not energetically possible for either product. Second, we observed that DCl products are predominantly backscattered; large background signals caused by contaminant HCl in our gas mixture prevented the measurement of HCl scattering. Finally, we observed that some DCl molecules were moving too slowly to result from the studied reaction. While we speculated on several effects that could contribute to formation of slow DCl, we were unable to resolve the issue quantitatively. The current study, which probes the methyl radical products, is able to make conclusive statements about product energy and scattering.

II. EXPERIMENT

Although the experimental apparatus is similar to that used for several previous publications,[1,2] we present here a

thorough overview. Methane (CH_4, Matheson, 99.97%; or CD_4, Cambridge Isotope Labs, 99% isotopic purity), molecular chlorine (Matheson research purity, 99.999%), and helium (Liquid Carbonic, 99.995%) are mixed in a Teflon™-lined steel tank. This gas mixture is then expanded into vacuum through a pulsed valve (General Valve 9-series, 0.6 mm orifice). Backing pressure is maintained at 200 Torr for measuring product velocity distribution or at 400 Torr to record methyl radical spectra. The lower backing pressure entails some loss of signal but improves instrumental resolution.

The reaction is initiated by photolysis of the molecular chlorine precursor at 305–375 nm. The photodissociation of Cl_2 is well characterized;[11] at these wavelengths, 96%–99% of the Cl atoms produced are in the ground $^2P_{3/2}$ electronic state. The tunable light for the photolysis is produced by a Nd^{3+}:YAG-pumped dye laser (Continuum PL9020 and ND6000) using DCM, LDS698, and LD700 laser dyes. The dye laser output is frequency doubled in a BBO crystal to produce 15–40 mJ pulses, which are gently focused into the gas expansion to a spot size of approximately 1 mm.

The reaction proceeds at a collision energy that is determined by the kinetic energy of the Cl reagent and by the translational temperature of the molecular beam. We have no direct measurement of the beam translational temperature; however, we have measured the rotational temperature of trace HCl in our expansion to be 15 K. We assume that this value is a reasonable upper bound for the translational temperature and calculate the collision energy spread accordingly.[12] Thus, for the $Cl+CH_4$ reaction we access collision energies from 1050 ± 160 to 1970 ± 220 cm^{-1}. For the $Cl+CD_4$ reaction, collision energies range from 1220 ± 170 to 2280 ± 230 cm^{-1}.

CH_3 and CD_3 products are detected using $2+1$ resonance-enhanced multiphoton ionization (REMPI) via the $3p_z$ Rydberg intermediate state; the 0_0^0 and 2_1^1 bands are at 333.9 and 330.7 nm for CD_3 and at 333.4 and 329.4 nm for CH_3.[13–15] A second frequency-doubled Nd^{3+}:YAG-pumped dye laser (Spectra Physics GCR 2A and PDL-3) operating with a mixture of DCM and LDS698 is used to generate the probe light. Detection is effected at the focal point of a 1.1 m lens, using 6–11 mJ/pulse of laser light. After ionization, the methyl ions traverse a time-of-flight (TOF) mass spectrometer and are detected using dual microchannel plates (MCPs) in a chevron configuration. The signal from the MCPs is recorded by a digital oscilloscope (Hewlett–Packard 54542A) and transferred to a personal computer.

Rotational spectra are recorded on the origin (0_0^0) vibrational band by tuning the REMPI laser and recording the total ion current for m/z of 15 (CH_3) or 18 (CD_3). For these measurements, the mass spectrometer is operated with high extraction fields in order to collect all product ions produced. Variations in probe laser power are small, and are measured simultaneously using a pyroelectric detector (Molectron J3). The recorded spectra are corrected for this variation assuming a quadratic power dependency for the ionization process. Measurement of vibrational branching is accomplished in a similar fashion through short scans over the vibrational bands of interest.

For measurement of product speed distributions, the probe laser is fixed on a rotational feature, usually the Q branch of the 0_0^0 band of the methyl radical. The mass spectrometer is then operated with a lower extraction field of 225 V/cm under Wiley–McLaren space-focusing conditions. The ionization process does not change the velocities of the detected products; thus, the ions are created with a distribution of speeds nearly identical to that of their neutral precursors. The packet of product ions then spreads as it traverses the mass spectrometer, according to the ion velocities. We obtain a one-dimensional projection of the ion packet by measuring the distribution of arrival times at the detector. Furthermore, we ''core extract'' the ion packet by placing a mask with a circular aperture directly before the detector, which serves to reject products with significant velocities perpendicular to the detection axis. The resulting ion arrival profile can be analyzed to yield the speed distribution of the reaction products, as has been reported in earlier publications.[16] The velocity sensitivity of the mass spectrometer was calibrated previously by measuring Cl atoms from Cl_2 photolysis over a range of excitation wavelengths.[16] In order to verify the calibration and optimize the mass spectrometer, ion arrival profiles for Cl atoms were recorded for each day of measurement.

Background signals for this experiment are relatively small. The major background results from the probe laser, and we attribute it to probe-induced photodissociation of Cl_2, followed by reaction within the time of the laser pulse, followed by detection of the methyl radical. Additionally, we observe minor background signals from multiphoton nonresonant dissociative ionization of methane, induced by both probe and photolysis lasers. Most backgrounds are corrected by a time-jump subtraction procedure, which is utilized for rotational spectra and for velocity measurements. In this subtraction, the time between the photolysis and probe lasers is varied between short (10 ns) and long (50–70 ns) delays, by directing the trigger pulse for the photolysis laser Q switch through varying coaxial cable lengths or by utilizing computer control of the timing electronics. This subtraction is performed either every other shot or every ten laser shots, and removes all background signals which are independent of photolysis/probe delay. Background ions produced by the photolysis laser alone are not compensated for by this procedure, but such background signals are small and produce characteristic early positive, late-negative difference signals that are easily identified and removed upon workup of the data.

The spatial anisotropy of the product velocities is determined by measuring how the ion arrival profiles depend on the direction of polarization of the photolysis laser. The chlorine atom reagent is created with a $\sin^2\theta$ spatial distribution with respect to the polarization vector, and the product spatial anisotropy is directly related to this, as no other sources of anisotropy exist in the experiment. The polarization of the photolysis laser light is controlled by synchronizing the experiment to a photoelastic modulator (Hinds International PEM-80), which is placed in the photolysis beam path. The linear polarization of the laser beam is flipped every other laser shot so as to lie parallel or perpendicular to the TOF

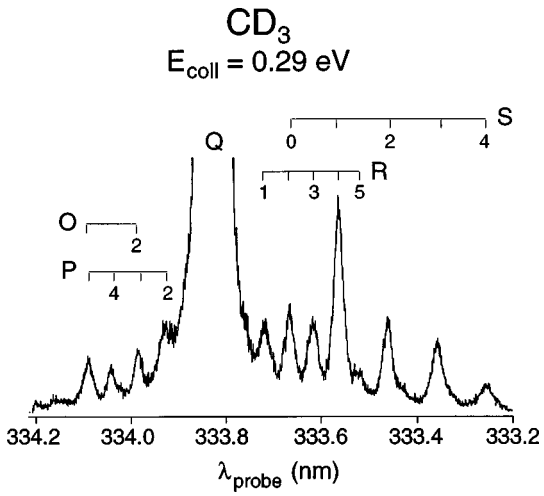

FIG. 1. Rotational spectrum for the CD_3 products of the $Cl+CD_4$ reaction at 0.29 eV collision energy, acquired on the 0_0^0 band connecting the ground state to the $3p_z$ state. Note that only several lines for each rotational branch have intensity, indicating that the reaction product has very little rotational energy.

axis, allowing ion arrival profiles to be acquired simultaneously for parallel and perpendicular photolysis geometries. We refer to these signals as $I_\parallel$ and $I_\perp$. Both lasers fire at 20 Hz repetition rates, so the experiment runs at 5 Hz, as it requires a four-state subtraction to account for two laser polarizations and two photolysis-probe time delays. Our experimental sensitivity to spatial anisotropy has been calibrated by observing Cl atoms from Cl_2 photodissociation.

III. RESULTS

A. CH_3 and CD_3 internal states and speed distributions

The rotational spectrum of the 0_0^0 band of CD_3 reaction products is shown in Fig. 1; the reagent collision energy is 0.29 eV. The spectrum is dominated by an intense *Q* branch, which is characteristic for a parallel transition in a symmetric top. In these scans, the *Q* branch was allowed to saturate our detection electronics in order to allow greater sensitivity for the weaker *O*-, *P*-, *R*-, and *S*-branch transitions. The considerable width of the rotational lines is indicative of the predissociative nature of the intermediate $3p_z$ Rydberg state. Spectra have been reported of methyl radicals resulting from a variety of sources that include pyrolysis and discharge sources,[13,17] flash-pyrolized jet-cooled radicals,[18] and radical products of photodissociation and reaction.[14,15,19–22] It is not straightforward to extract rotational populations from the spectral data. Such an analysis requires knowledge of the predissociation dynamics of the intermediate Rydberg state and the nuclear spin populations of the methyl radicals, and often involves assumption of thermal distributions of *J* and *K* states. The paucity of observed rotational lines in our spectra, which is compounded by systematic overlaps between *O* and *P* branches and *R* and *S* branches, makes a population analysis infeasible. Furthermore, because we are probing nascent reaction products, it is quite possible for populations of *J* levels and *K* sublevels to be highly nonthermal due to dynamical considerations. However, we can glean two significant facts from this methyl radical spectrum. First, the spectra shown in Fig. 1 show less rotational excitation than spectra reported in any of the aforementioned studies, indicating that the CD_3 products from $Cl+CD_4$ are extremely rotationally cold. Second, we observe that *S*-branch transitions are more intense than corresponding *R*-branch transitions. [Compare $S(1)$ and $R(1)$, for example, or note that $S(2)$ is larger than $R(2)$, even though the latter is overlapped with $S(0)$.] By examining symmetric top two-photon line strengths, we can deduce that the methyl radical products are formed preferentially in lower *K* sublevels. We have made similar measurements of the spectrum of CH_3, which also appears to have very little rotational energy.

We were able to detect the CH_3 ($\nu_2=1$) product via the 2_1^1 band. The total intensity of this band (integrated over all rotational lines from 329.7 to 329.2 nm) was 48 ± 12 times smaller than that of the 0_0^0. We conclude that nearly all of the products are formed vibrationless, with only a small amount of umbrella-bending (ν_2) excitation. A similar measurement for CD_3 was not able to observe the 2_1^1 band, establishing an upper limit for the band intensity that is 40 times smaller than the origin band. Theoretical Franck–Condon factors were used in order to relate CH_3 and CD_3 REMPI intensities to vibrational populations,[14,19,23] resulting in a ratio of sensitivities of 1.1 for the 0_0^0 and 2_1^1 transitions for both isotopomers. We conclude that the population of CH_3 ($\nu_2=1$) is $2.3\%\pm0.6\%$, and the population of CD_3 ($\nu_2=1$) is less than 3%.

Core-extracted ion arrival profiles are acquired with the photolysis laser polarization vector parallel and perpendicular to the time-of-flight axis. These profiles, which are referred to as $I_\parallel$ and $I_\perp$, are appropriately summed ($I_{iso}=I_\parallel+2I_\perp$) to remove the effects of spatial anisotropy arising from the Cl_2 photodissociation. This isotropic composite profile, I_{iso}, is related to the product speed distribution alone. Speed distributions are inverted from the isotropic ion arrival profiles using a maximum entropy analysis that is detailed in earlier publications.[16] Figure 2 shows the isotropic profiles and resulting speed distributions for the CD_3 product of the $Cl+CD_4$ reaction. Error bars for the speed distribution are 1σ standard deviations from statistical analysis of replicate measurement. These data are acquired with photolysis wavelengths of 307, 320, 335, 355, and 375 nm, corresponding to center-of-mass collision energies of 0.28, 0.25, 0.22, 0.18, and 0.15 eV. Figure 3 shows isotropic profiles and speed distributions for the CH_3 product of the $Cl+CH_4$ reaction. These data are acquired using the same five photolysis wavelengths, which correspond to slightly lower center-of-mass collision energies of 0.24, 0.22, 0.19, 0.16, and 0.13 eV. The small features visible on the baseline of the ion arrival profiles are background signals resulting from ionization of methane by the photolysis laser, and they do not impact analysis of the data.

The shaded areas under the speed distributions shown in Figs. 2 and 3 indicate the methyl radical product speeds which are moving faster than energetically possible for the ground-state reaction. These limits are calculated by determining the center-of-mass frame speed of the methyl radical from conservation of energy, given our previous measure-

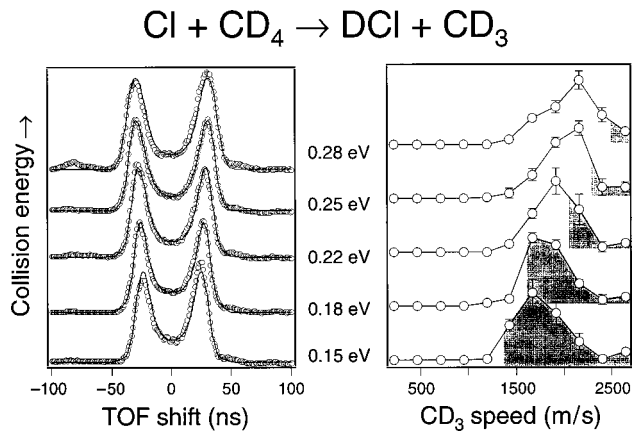

FIG. 2. Core-extracted ion arrival profiles for the CD_3 product of the $Cl+CD_4$ reaction and a fit (the solid line) to the data, along with speed distributions resulting from the fit. The profiles are isotropic composite profiles which are independent of the photolysis laser polarization; they are acquired on the *Q* branch of the origin band at reagent collision energies of 0.15, 0.18, 0.22, 0.25, and 0.28 eV. The shaded area under each speed distribution indicates the product speeds which are greater than energetically possible for products of the ground-state $Cl+CD_4$ reaction. Note that at all collision energies, some products are moving at anomalously fast speeds; this effect is particularly pronounced at low collision energies.

ment of virtually no internal excitation of the HCl (DCl) partner,[3] and using endothermicities of 0.07 and 0.11 eV for the $Cl+CH_4$ and $Cl+CD_4$ reactions. For every speed distribution measured, some of the products are moving faster than the maximum allowable speed. This effect is minor for high collision energies but is quite pronounced at the lowest collision energies. Additionally, the presence of products moving too quickly is more noticeable for CD_3 than for CH_3. At the lowest collision energy studied, 0.15 eV, virtually all of the CD_3 radicals have too much kinetic energy to be products of the $Cl+CD_4$ reaction.

B. Explanation of anomalously fast products

We attribute the anomalously fast methyl radical products to the reaction of chlorine with vibrationally excited

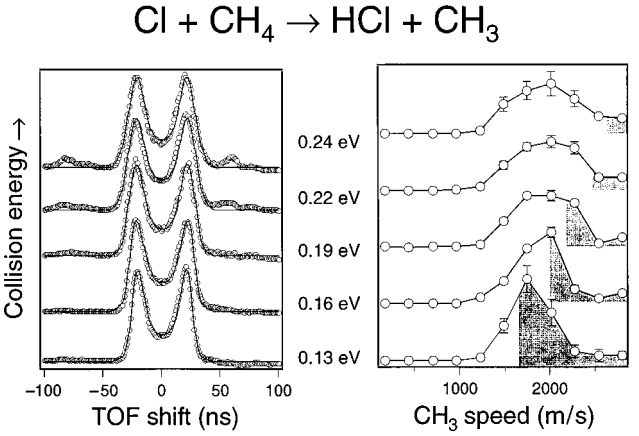

FIG. 3. Core-extracted ion arrival profiles and speed distributions for the CH_3 product of the $Cl+CH_4$ reaction. The data are analogous to that presented in Fig. 2, and are acquired for collision energies of 0.13, 0.16, 0.19, 0.22, and 0.24 eV.

methane, and we make the case for this hypothesis first. Subsequently, we will explain how other effects, such as translational energy spread between the reagents or inaccuracy in determining product energies or reaction energetics, cannot create the observed speed distributions; we will also discuss the possibility of the reaction of spin–orbit-excited chlorine atoms. Section III C will detail how spatial anisotropy measurements are used to verify our hypothesis of vibrationally excited reaction and discount reaction of excited chlorine atoms.

We propose that some of the CH_4 and CD_4 reagents are vibrationally excited in either the bending (ν_4) or torsional (ν_2) modes, and that the reaction of chlorine with these vibrationally excited reagents leads to the production of methyl radicals with too much energy to result from reaction with ground-state methane. In CD_4, these vibrational modes have roughly 1000 cm^{-1} of energy and a thermal population of 4% at 300 K; in CH_4, the vibrational modes have 1400 cm^{-1} of energy and a population of 0.7% at 300 K.[24] We would not expect our relatively gentle molecular expansion to relax vibration significantly. While methane reagents should be translationally and rotationally cold, vibrational populations should remain near thermal values. Previous studies have shown that C–H stretch (ν_3) excitation significantly enhances reactivity in the $Cl+CH_4$ reaction;[3,7] we posit that bending and/or torsional excitation could enhance reactivity in a similar fashion. Thus, the small population of vibrationally excited methane could lead to a sizable fraction of the products. Furthermore, we note that the excess vibrational energy in the methane reagent is adequate to explain all observed methyl radical product velocities. The effect of the vibrationally enhanced reaction would be most noticeable at low collision energies, where the reaction with ground-state methane is near or below threshold. We observe more anomalously fast methyl radicals at low collision energies, in accordance with this explanation. This effect is more pronounced for reaction with CD_4 than for CH_4, which can be explained by the higher vibrational populations of the perdeuterated isotopomer.

We discuss other sources of anomalously fast methyl radical products. Inaccuracy in estimating product internal energies is unlikely, as the state-specific nature of our detection process precludes significant error. Similarly, the thermodynamics of the $Cl+CH_4$ reaction are well enough known to rule out error in energetics as a relevant factor. Consequently, excess kinetic energy in the methyl radical products necessarily results from extra energy in the reagents. We posited significant reactivity for vibrationally excited reagents present in the beam, as described in the preceding paragraph. Another possible source of fast methyl radical products is from reaction with electronically excited chlorine atoms. Excited chlorine, $Cl\ ^2P_{1/2}$ or Cl*, has 881 cm^{-1} of energy and is produced in Cl_2 photodissociation with populations that are wavelength dependent and range from 1% at 300 nm photolysis to 4% at 375 nm.[11] As mentioned previously, as the reaction nears threshold at lower collision energies, this small amount of excited reagents could contribute significantly in product formation. Furthermore, the enhanced reactivity of Cl* has been proposed as a mechanism

to explain anomalies in rate measurements of hydrocarbon reactions.[25] It might seem difficult to distinguish products resulting from reaction with vibrationally excited methane from those resulting from electronically excited chlorine. However, ground-state chlorine is produced via a perpendicular dissociative transition in Cl_2, and thus the fragments are produced in a $\sin^2\theta$ distribution, where θ is the angle between the recoil direction and the photolysis laser polarization. Cl* is produced via a parallel transition and is produced in a $\cos^2\theta$ distribution. Products resulting from reaction with Cl* are therefore experimentally resolvable from those resulting from reaction with ground-state chlorine, and we will detail these measurements presently.

A third possibility is that spread in translational energy of the reagents could result in increased collision energy and thus fast products. We expect our molecular expansion to be translationally cold and generally assume a translational temperature of 15 K. This residual thermal motion leads to a spread of $\pm 170\ cm^{-1}$ at $1220\ cm^{-1}$ collision energy, and as the reaction nears threshold, a disproportionate number of products could result from the high end of this distribution. However, the spread in collision energy is caused almost entirely by the motion of the lighter CH_4 or CD_4 reagent. Collisions at the high end of our thermal spread are those in which the methane is moving toward the chlorine atom, and while these collisions have more energy available for products, they also have a reduced center-of-mass velocity. Consequently, such processes do not produce significantly faster methyl radical products, and can be ruled out as a source of the observed effect in our speed distributions.

C. Spatial anisotropy measurements and differential cross sections

Further evidence for enhanced reactivity of thermally populated vibrational modes of CD_4 and CH_4 is available in a measurement of the product spatial anisotropy; in addition, spatial anisotropy measurements can rule out large contributions to reactivity from Cl*. All spatial anisotropy in the experiment is derived from the photodissociation. Ground-state chlorine atoms are formed with a $\sin^2\theta$ distribution (characterized by a spatial anisotropy parameter, $\beta=-1$); excited-state chlorine atoms are formed, at longer photolysis wavelengths, with a $\cos^2\theta$ distribution ($\beta=2$). In reactive collisions where the methyl radical product velocity is parallel to the chlorine reagent velocity (forward- and backward-scattered products), the spatial distribution of the products will be equal to that of the reagents. When the product and reagent velocities deviate by an angle α, the product spatial distribution is reduced by $P_2(\cos\alpha)$. The resulting product spatial anisotropy can be calculated from the center-of-mass scattering angle and the reaction kinematics; thus, a measurement of the product spatial anisotropy can be used to determine the kinematics of a reaction. Figure 4 demonstrates this behavior; it shows Newton diagrams for $Cl+CH_4$ ($v=0$) and $Cl+CH_4$ (ν_2 or $\nu_4=1$). CH_3 products of the ground-state reaction have relatively little translational energy available in the center-of-mass frame, resulting in the small Newton circle in Fig. 4(a). The lab-frame velocities of the products therefore will always be near parallel to the chlorine

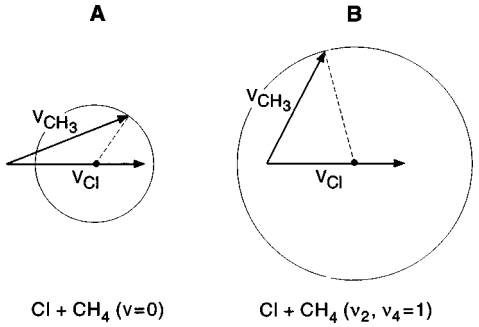

FIG. 4. Newton diagrams for (a) $Cl+CH_4$ ($v=0$) and (b) $Cl+CH_4$ (ν_2 or $\nu_4=1$) at 0.16 eV collision energy. (a) The products of the ground-state reaction have velocities that are constrained to lie within 40° of the chlorine reagent velocity. (b) The greater amount of energy available in the vibrationally excited reaction allows more deviation of the product and reagent velocities. The greatly different sizes of the Newton circles for the two reactions thus allows a measurement of product spatial anisotropy so that it is possible to distinguish experimentally between the two processes (see the text).

atom reagent velocity, with $\mathbf{v}_{Cl}$ and $\mathbf{v}_{CD_3}$ deviating by a maximum of 40°, resulting in a spatial anisotropy which can range from -0.3 to -1.0. Products of the vibrationally excited reaction, $Cl+CH_4$ (ν_2 or $\nu_4=1$), have significantly more translational energy, as shown by the larger Newton circle in Fig. 4(b), and have velocities which deviate by as much as 90° from the chlorine velocity; product spatial anisotropy can thus range from $+0.5$ to -1.0. We have employed a similar treatment of product spatial distribution measurements to estimate product C_2H_5 internal energy in the $Cl+C_2H_6$ reaction and product CH_3 internal energy in the $Cl+CH_4$ ($\nu_3=1$) reaction.[1,2,7]

Experimental core-extracted ion arrival profiles are use to construct anisotropic composite profiles, $I_{aniso}=2(I_{\parallel}-I_{\perp})$. Figure 5 presents sample anisotropic profiles for CD_3

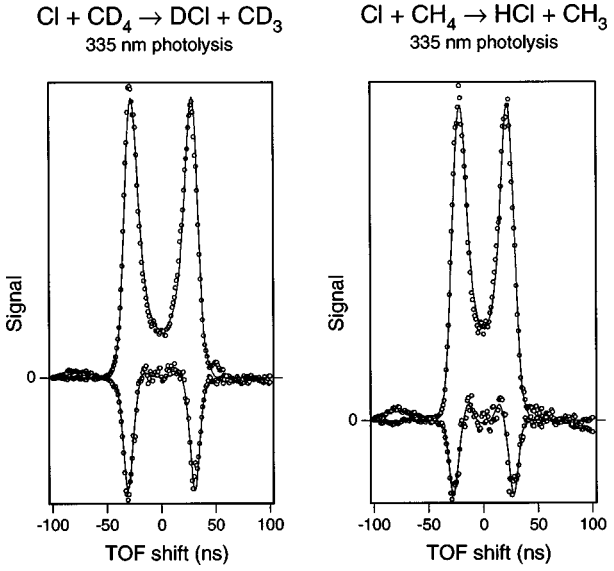

FIG. 5. Anisotropic core-extracted ion-arrival profiles for CD_3 and CH_3 products at 0.22 and 0.19 eV collision energies. The anisotropic profiles are shown along with the corresponding isotropic profile for scaling purposes. A least-squares fit to the profile produces the speed-dependent spatial anisotropy of the product, $\beta(v)$.

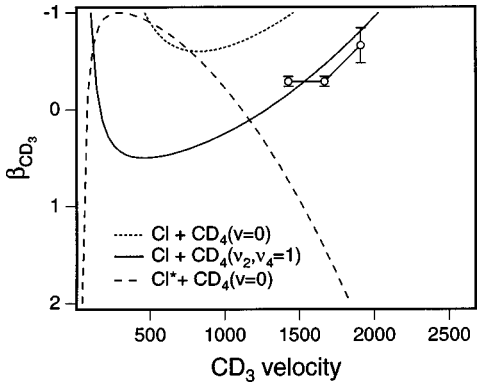

FIG. 6. Speed-dependent spatial anisotropy for CD_3 products at the lowest collision energy studied, 0.15 eV. The data are presented along with three curves showing the predicted spatial anisotropy for the ground-state reaction (the dotted line), reaction with CD_4 (ν_2 or $\nu_4=1$) (the solid line), and reaction of Cl* (the dashed line). The data indicate that reaction with vibrationally excited methane is the dominant process at this collision energy; no combination of the other two curves would be adequate to fit the data.

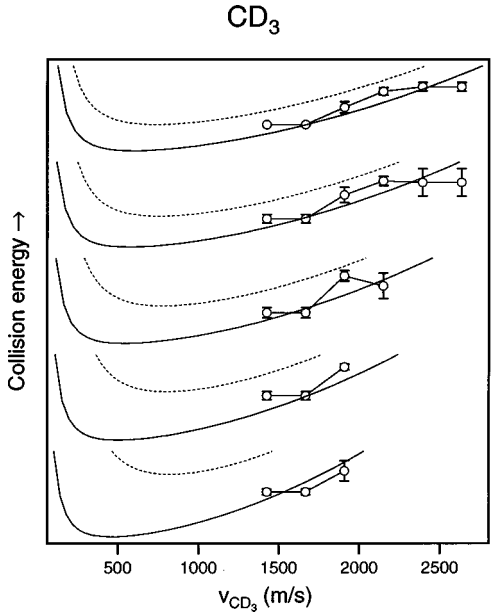

FIG. 7. Speed-dependent spatial anisotropies for CD_3 products at collision energies of 0.15, 0.18, 0.22, 0.25, and 0.28 eV, plotted along with curves showing the predicted anisotropy for ground-state and vibrationally excited reaction at each collision energy; the plot is similar to that shown in Fig. 6, with data for each of the five collision energies stacked vertically. At low collision energy, the data are fit entirely by the solid curve, corresponding to reactivity of vibrationally excited reagents only. As collision energy increases, the spatial anisotropy tends to lie increasingly between the solid and dashed curves, indicating that both processes are taking place. Note that the data are never fit solely by the dashed, ground-state curve, as even at the highest collision energies studied, vibrationally excited CD_4 contributes to reactivity.

and CH_3 products, shown along with the isotropic profiles for scaling purposes. The fits shown are those obtained through a nonlinear least-squares procedure; to reduce covariance, the number of basis functions was reduced from the number used for the speed distribution fit. The result of the fit is $\beta(v)$, the spatial anisotropy as a function of product speed. Figure 6 shows $\beta(v)$ for CD_3 at the lowest collision energy studied, 0.16 eV. At this energy, all observed products are moving too quickly to have resulted from the ground-state reaction. The measured spatial anisotropy is plotted along with three calculated curves, which show the predicted $\beta(v)$ values for the ground-state reaction, for reaction with vibrationally excited CD_4 (ν_2 or ν_4), and for reaction of electronically excited chlorine. The ground-state reaction should have $\beta(v)$ as shown by the dotted curve, with values of β closest to -1, as there is very little energy in the center-of-mass frame available for product translation. The solid curve, corresponding to the vibrationally excited reaction, shows how the excess energy in the reagent results in a wider range of values for β. The dashed curve results from the opposite spatial anisotropy ($\beta=2$) of the Cl* reagent. The solid curve provides an exceedingly good match to the data, whereas no combination of the other two curves can provide a reasonable fit to the measured anisotropy. Thus, we conclude that at 0.16 eV collision energy, all products result from reaction with vibrationally excited CD_4. There is no evidence for reaction of Cl $^2P_{1/2}$. Because the concentration of the Cl* reagent is low (4%), we cannot conclude that electronically excited chlorine is generally unreactive; however, because the signal is dominated by the enhanced reactivity of trace vibrationally excited species, we can state that any enhancement of the Cl* reaction rate is small in comparison.

Figures 7 and 8 show speed-dependent spatial anisotropies, derived from the analysis of anisotropic profiles, for CD_3 and CH_3, respectively. The data were acquired at the same collision energies reported for the data of Figs. 2 and 3, and are shown along with calculated $\beta(v)$ curves for the ground-state and vibrationally excited reactions. As discussed in the previous paragraph, the lowest collision energy for $Cl+CD_4$ results in reactivity of vibrationally excited species only. At higher collision energies, the spatial anisotropy data lie between the solid and dashed curves, indicating that both ground-state and vibrationally excited reactions are taking place. For the $Cl+CH_4$ reaction, the data indicate a larger proportion of ground-state reactivity as compared to $Cl+CD_4$; this is likely caused by the decreased population of CH_4 vibrational modes. It is important to note that even for the highest collision energies, the spatial anisotropy data never lie completely on the $\beta(v)$ curve predicted for the ground-state reaction. It appears that reagent vibrational excitation results in significant enhancement of reactivity even for collision energies far above threshold. This effect will be discussed in detail in Sec. IV.

The speed-dependent spatial anisotropy can be used to deconvolute the speed distributions of the ground-state and vibrationally excited reactions. Sufficient data exist, therefore, to calculate the differential cross sections for each reaction and to determine the relative reactivities of the two processes. However, such an approach would extend the analysis beyond the capabilities of the data to support, given the resolution and error bars of the measurements. Instead, we present a more qualitative analysis. We note that for any given collision energy, the measured spatial anisotropy lies between the values calculated for ground-state and vibrationally excited reactions in a generally speed-independent fashion. Thus the speed distributions for the products of

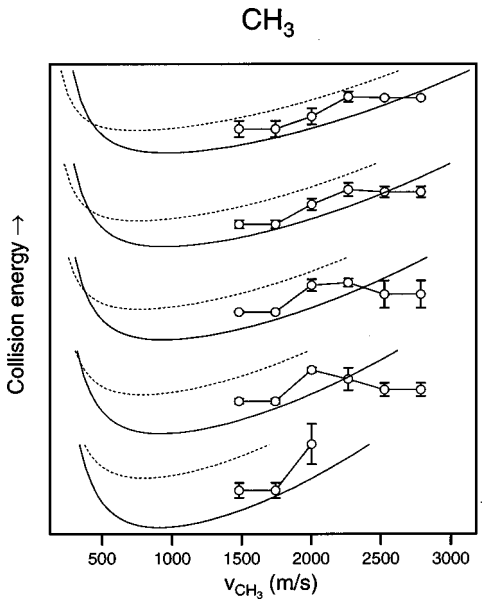

FIG. 8. Speed-dependent spatial anisotropies for CH_3 products at collision energies of 0.13, 0.16, 0.19, 0.22, and 0.24 eV, plotted similarly to Fig. 7. The data show that both ground-state and vibrationally excited reactions are taking place, though the proportion of ground-state reactivity is higher for $Cl+CH_4$ than for $Cl+CD_4$, presumably due to the decreased population of vibrational modes.

ground-state and vibrationally excited reactions are fairly similar, with the exception of the anomalously fast products. We assume that the measured product speed distribution is characteristic for both reactions (after truncating the anomalously fast products), and we invert this single speed distribution to give differential cross sections for both processes. Insofar as the spatial anisotropy data tend to follow the $\beta(v)$ contours, we expect our resulting differential cross sections to be qualitatively correct for both ground- and excited-state reactions.

Figures 9 and 10 show differential cross sections for CD_3 and CH_3 products for both vibrationally excited and ground-state reactions. We note that there is a general trend in the spatial anisotropy measurements which favors the vibrationally excited reaction at slower speeds. Consequently, we expect the actual differential cross sections to be slightly more backscattered for the vibrationally excited reaction, and slightly more forward scattered for the ground-state reaction. Figure 9 shows that CD_3 from $Cl+CD_4$ ($v=0$) is sharply forward scattered at low collision energy. This result implies that the corresponding DCl product is sharply backscattered, in agreement with previous measurements.[3] As collision energy increases, the products become more side scattered, though they always remain forward peaked. Scattering for $Cl+CD_4$ (ν_2 or $\nu_4=1$) is generally side scattered and does not change significantly with collision energy. Similarly, Fig. 10 shows that CH_3 products from $Cl+CH_4$ ($v=0$) are forward scattered at low collision energy. Side scattering increases with collision energy, so that unlike CD_3 products, CH_3 is predominantly side scattered at high energies. Vibrationally excited CH_4 (ν_2 or $\nu_4=1$) produces forward- and side-scattered products, largely independent of collision energy.

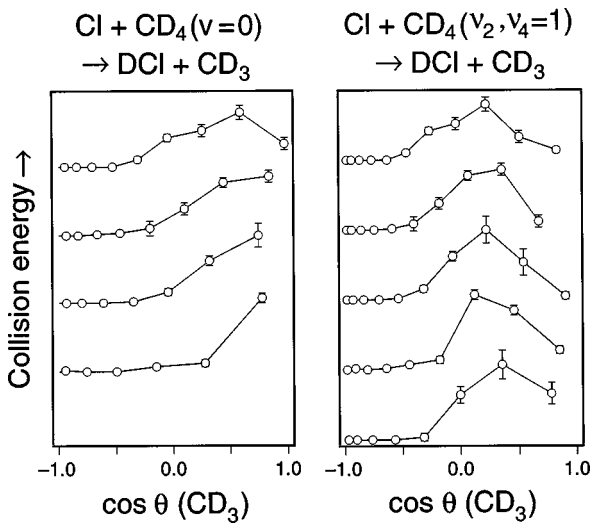

FIG. 9. Differential cross sections for $Cl+CD_4$ ($v=0$) and $Cl+CD_4$ (ν_2 or $\nu_4=1$) showing the methyl product angular distributions at reagent collision energies of 0.15, 0.18, 0.22, 0.25, and 0.28 eV. The cross sections are deconvoluted from the speed distributions shown in Fig. 2 in a qualitative manner that is detailed in the text.

We assume that vibrational populations in our expansion are very close to thermal values. We conclude with qualitative estimates of the relative reactivity of ground- and excited-state methane, and note that as we cannot distinguish between ν_4 and ν_2 reactivity, we are sensitive only to the average reactivity of the two modes. At 0.15 eV collision energy, all observed CD_3 products come from the vibrationally excited reaction. At higher collision energy, the relative rate of the ground-state reaction increases, so that by 0.28 eV, approximately 75% of the products result from CD_4 ($v=0$), implying an 80 times greater reactivity for CD_4 (ν_2 or $\nu_4=1$). For $Cl+CH_4$, 75% of the products come from the ground-state reaction at 0.13 eV collision energy, and 60% of the products at 0.24 eV; this behavior allows the rough

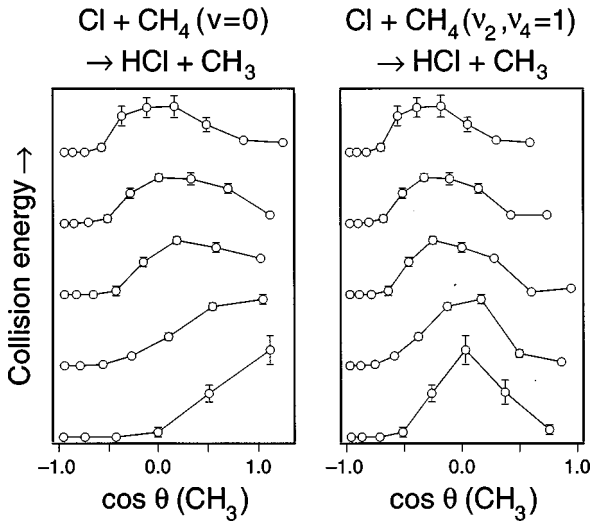

FIG. 10. Differential cross sections for $Cl+CH_4$ ($v=0$) and $Cl+CH_4$ (ν_2 or $\nu_4=1$) at collision energies of 0.13, 0.16, 0.19, 0.22, and 0.24 eV.

estimate that the vibrationally excited species is 400 and 200 times more reactive at these two collision energies, respectively.

IV. DISCUSSION

We have studied the CH_3 and CD_3 radical products of the $Cl+CH_4$ and $Cl+CD_4$ reactions, varying the collision energy between 0.13 and 0.29 eV. These products are formed with very little energy in vibration or rotation. Core-extracted ion arrival profiles were measured to obtain speed and spatial anisotropy distributions of the methyl radical products. The speed distributions contain products moving at anomalously fast speeds that could not originate from the $Cl+CH_4$ ($v=0$) or $Cl+CD_4$ ($v=0$) reactions. We attribute these products to the reaction of trace amounts of vibrationally excited methane in our expansion, with the excited methane belonging to one or both low-lying thermally populated bending and torsional modes (ν_2 or ν_4). Product spatial anisotropy measurements were used to verify this hypothesis. These low-energy vibrations result in a large enhancement of reactivity; at the highest collision energy studied, CD_4 (ν_2 or $\nu_4=1$) is 80 times more reactive than CD_4 ($v=0$), and CH_4 (ν_2 or $\nu_4=1$) is 200 times more reactive than CH_4 ($v=0$). At low collision energies, where the reaction of chlorine with ground-state methane should be near or below threshold, vibrationally excited reagents dominate reactivity. Spatial anisotropy measurements were additionally used to discount the possibility of enhanced reaction of electronically excited chlorine, for which we see no experimental evidence. We perform a qualitative deconvolution of product scattering for ground-state and vibrationally excited reactions. Products of the vibrationally excited reaction are side scattered and vary little with reaction collision energy. Products of the ground-state reaction are forward scattered at low collision energies and show increased side scattering at higher collision energies.

We will first discuss the reaction of chlorine with ground-state methane in terms of the line-of-centers model, which qualitatively describes the scattering and collision energy dependence of the reaction products. We will then compare the state and scattering distributions for the vibrationally excited reaction to earlier studies of the reaction of chlorine with C–H stretch-excited methane. We relate our results to the theoretical work of Duncan and Truong,[26] which is relevant to both ground-state and excited-state reactions. Finally, we will detail how vibrational enhancement is expected to affect the thermal kinetics of the reaction of chlorine with methane.

Earlier studies of $Cl+CD_4$ ($v=0$) and $Cl+C_2H_6$ ($v=0$) explained product scattering qualitatively in terms of the line-of-centers model,[2,3] which states that only the component of translational energy which lies along the line connecting the reagents' centers of mass can be used to surmount the barrier to reaction. Using this model, the large barrier and relatively small collision energy for the $Cl+CD_4$ ($v=0$) reaction would constrain only the most direct of collisions to lead to reactions, whereas the small barrier for $Cl+C_2H_6$ ($v=0$) would allow glancing collisions to produce products, as well. By assuming that the products scatter in the same manner as hard spheres, we predict that $Cl+CD_4$ ($v=0$) should produce backscattered DCl (and thus forward-scattered CD_3), while $Cl+C_2H_6$ ($v=0$) should produce isotropically scattered products. Both of these predictions are in accord with our observations. Furthermore, the line-of-centers model states that with increasing collision energy, more glancing collisions become reactive, which would lead to an increase in product side scattering, as is observed in this study. $Cl+CH_4$ ($v=0$), while similar to the perdeuterated reaction, is not as well explained by this qualitative model. At 0.22 eV collision energy, scattering for CH_3 peaks in the sideways direction and decreases in both forward and backward directions, and presumably, $Cl+CD_4$ ($v=0$) would show similar behavior at higher collision energies. While the simple, classical model explains the gross behavior of the ground-state reaction, evidently more involved dynamical effects are in play.

Our previous studies of the $Cl+CH_4$ ($\nu_3=1$) reaction showed that the asymmetric C–H stretching mode dramatically impacts reactivity. We observed through a direct measurement that ν_3 excitation increases reactivity by a factor of 30 at 0.16 eV collision energy.[3] In light of the present results, approximately 75% of products which we attributed to ground-state reaction should in fact result from reaction of CH_4 (ν_2 or $\nu_4=1$), and therefore the enhancement of reactivity caused by ν_3 excitation is closer to 120. Our model for the $Cl+CH_4$ ($\nu_3=1$) reaction stated that the reagent vibrational excitation fully opens the cone of acceptance for the reaction, i.e., nearly all reagent collisions result in products. The similar reactivity of the bending and/or torsional modes indicates that smaller amounts of vibrational energy are sufficient to promote reaction for most collisions. Additionally, the scattering deduced for $Cl+CH_4$ (ν_2 or $\nu_4=1$) is similar to the broad side scattering measured for the HCl ($v=0$) product of $Cl+CH_4$ ($\nu_3=1$). Product state distributions, however, are markedly different, as $Cl+CH_4$ ($\nu_3=1$) yields products with significant rotational and vibrational excitation.

Duncan and Truong[26] published a transition-state-theory analysis of the $Cl+CH_4$ reaction which calculated thermal rates for CH_4 with bending (ν_4) and stretching (ν_1) mode excitation.[26] This study reported significantly enhanced rates from excitation of either vibrational mode, due to a lowering or a removal of the barrier to reaction. For the reverse reaction, $CH_3+HCl \rightarrow CH_4+Cl$, vibrational excitation of the CH_3 reagent had small to negative effects on reaction rate. The calculated rates are in agreement with the lack of methyl radical vibrational excitation reported in this paper. Because methane is tetrahedral and methyl radical is planar, a Franck–Condon type of argument would predict significant umbrella-bending excitation of the methyl product of this reaction, in contrast to the measured result. However, the large enhancement in reactivity seen for CH_4 ($\nu_4=1$) suggests that umbrella bending lies along the reaction coordinate, and the transition state for the reaction occurs when the methyl is in a more planar geometry. Thus, while projecting the methane geometry onto the methyl radical would indeed imply product bending excitation, this geometry would very rarely lead to reaction. This model is the traditional one of a

reaction with a ''late'' transition state, in which the transition state resembles the reaction products, and a productlike transition state has indeed been calculated theoretically for $Cl+CH_4$.[26,27] In such systems, vibrational energy enhances reactivity, whereas translational energy is generally ineffective; furthermore, products of such reactions are generally formed with small amounts of vibration and large amounts of translation. Our previous studies of HCl and DCl include measurements of total reactivity,[3] scattering,[3,7] and product rotational alignment,[4,6] all of which indicate a reaction pathway which is ''late'' with respect to C–H stretching. The current study indicates the transition state is also productlike with respect to methyl radical bending.

It is well known that $Cl+CH_4$ displays non-Arrhenius behavior; i.e., the thermal reaction rate as a function of temperature cannot be described accurately as a simple exponential, $k(T)=Ae^{-E_a/kT}$. Our present study reports enhancement in reactivity due to excitation of low-lying vibrational modes. It is likely that this vibrational enhancement has a substantial effect in the thermal kinetics of the reaction. The population of excited CH_4 vibrational modes is 0.7% at room temperature but increases to 30% at 800 K. Enhancement of reactivity from vibrational excitation of methane therefore causes an increase in reaction rate at high temperatures, which is in accordance with the observed kinetic data. At low temperatures, the ground-state reaction dominates reactivity, and we expect that fits to the low-temperature data would produce an accurate activation energy for the reaction which is lower than that calculated for a larger temperature range. In order to test this model we constructed a simple fit to the rate data by assuming that the individual ground-state and excited-state reactions each produced an exponential dependence of rate on temperature. We produced an excellent fit to the data using a ground-state activation energy of 700 cm^{-1}, an excited-state activation energy several hundred cm^{-1} lower, and a preexponential factor for the vibrationally excited reaction that was approximately 10 times larger than that of the ground-state reaction. We do not present these numbers as quantitative, but we note that they are reasonable from a dynamical standpoint and thus support the plausibility of our explanation. Thus, the enhanced reactivity of chlorine with methane having vibrational excitation in its low-lying bending or torsional modes should be an important factor in accounting for its kinetics under thermal conditions.

ACKNOWLEDGMENTS

S.A.K. thanks the National Science Foundation for a predoctoral fellowship. S.A.K. also gratefully acknowledges receipt of a Dr. Franklin Veatch Memorial fellowship. This work has been supported by the National Science Foundation under Grant No. CHE-93-22690.

[1] S. A. Kandel, T. P. Rakitzis, T. Lev-On, and R. N. Zare, J. Phys. Chem. A **102**, 2270 (1998).
[2] S. A. Kandel, T. P. Rakitzis, T. Lev-On, and R. N. Zare, J. Chem. Phys. **105**, 7550 (1996).
[3] W. R. Simpson, T. P. Rakitzis, S. A. Kandel, T. Lev-On, and R. N. Zare, J. Phys. Chem. **100**, 7938 (1996).
[4] T. P. Rakitzis, S. A. Kandel, T. Lev-On, and R. N. Zare, J. Chem. Phys. **107**, 9392 (1997).
[5] S. A. Kandel, T. P. Rakitzis, T. Lev-On, and R. N. Zare, Chem. Phys. Lett. **265**, 121 (1997).
[6] A. J. Orr-Ewing, W. R. Simpson, T. P. Rakitzis, S. A. Kandel, and R. N. Zare, J. Chem. Phys. **106**, 5961 (1997).
[7] W. R. Simpson, T. P. Rakitzis, S. A. Kandel, A. J. Orr-Ewing, and R. N. Zare, J. Chem. Phys. **103**, 7313 (1995).
[8] R. Atkinson, D. L. Baulch, R. A. Cox, R. F. Hampson, Jr., J. A. Kerr, and J. Troe, J. Phys. Chem. Ref. Data **21**, 1125 (1992).
[9] J. S. Pilgrim, A. McIlroy, and C. A. Taatjes, J. Phys. Chem. A **101**, 1873 (1997).
[10] W. B. DeMore *et al.* Evaluation No. 11, JPL Publication, No. 94-26; Jet Propulsion Laboratory, Pasadena, CA, 1994.
[11] Y. Matsumi, K. Tonokura, and M. Kawasaki, J. Chem. Phys. **97**, 1065 (1992).
[12] W. J. van der Zande, R. Zhang, R. N. Zare, K. G. McKendrick, and J. J. Valentini, J. Phys. Chem. **96**, 8205 (1991).
[13] J. W. Hudgens, T. G. DiGiuseppe, and M. C. Lin, J. Chem. Phys. **79**, 571 (1983).
[14] D. H. Parker, Z. W. Wang, M. H. M. Janssen, and D. W. Chandler, J. Chem. Phys. **90**, 60 (1989).
[15] R. O. Loo, G. E. Hall, H.-P. Haerri, and P. L. Houston, J. Phys. Chem. **92**, 5 (1988).
[16] W. R. Simpson, A. J. Orr-Ewing, S. A. Kandel, T. P. Rakitzis, and R. N. Zare, J. Chem. Phys. **103**, 7299 (1995).
[17] J. Heinze, N. Heberle, and K. Kohse-Höinghaus, Chem. Phys. Lett. **223**, 305 (1994).
[18] P. Chen, S. D. Colson, W. A. Chupka, and J. A. Berson, J. Phys. Chem. **90**, 2319 (1986).
[19] R. O. Loo, H.-P. Haerri, G. E. Hall, and P. L. Houston, J. Chem. Phys. **90**, 4222 (1989).
[20] D. Chandler, J. Thoman, M. Janssen, and D. Parker, Chem. Phys. Lett. **156**, 151 (1989).
[21] D. W. Chandler, M. H. Janssen, S. Stolte, R. N. Strickland, J. W. Thoman, and D. H. Parker, J. Phys. Chem. **94**, 4839 (1990).
[22] R. Schott, J. Schlütter, M. Olzmann, and K. Kleinermann, J. Chem. Phys. **102**, 8371 (1995).
[23] P. Botschwina, J. Flesch, and W. Meyer, Chem. Phys. **74**, 321 (1983).
[24] G. Herzberg, *Infrared and Raman Spectra of Polyatomic Molecules* (Van Nostrand, Toronto, 1966), Vol. 2.
[25] A. R. Ravishankara and P. H. Wine, J. Chem. Phys. **72**, 25 (1980).
[26] W. T. Duncan and T. N. Truong, J. Chem. Phys. **103**, 9642 (1995).
[27] T. N. Truong, D. G. Truhlar, K. K. Baldridge, M. S. Gordon, and R. Steckler, J. Chem. Phys. **90**, 7137 (1989).